$Co^{III}P^{2+}$ radicals average[14,31] ~6–7 g to be compared with the ~3 G found here in the a_{1u} Co species.) Negative spin densities at the nitrogen atoms, expected for a_{1u} porphyrins,[14] or some admixture of a_{2u} character,[16,44] may provide the mechanism that couples metal and radical in compounds I of chloroperoxidase and other presumed a_{1u} species.

(44) Morishima, I.; Takamuki, Y.; Shiro, Y. *J. Am. Chem. Soc.* **1984**, *106*, 7666–7672.

Acknowledgment. This work was supported by the Division of Chemical Sciences, U.S. Department of Energy (Contract DE-AC02-76CH00016) at Brookhaven National Laboratory and by the National Science Foundation at Michigan State University.

Biomimetic Models for Cysteine Proteases. 3. Acylation of Imidazolium–Thiolate Zwitterions by *p*-Nitrophenylacetate as a Model for the Acylation Step and Demonstration of Intramolecular General-Base-Catalyzed Delivery of H_2O by Imidazole to Thiol Esters as a Model for the Deacylation Step

J. P. Street,[†] K. I. Skorey,[†] R. S. Brown,*[†] and R. G. Ball[‡]

Contribution from the Department of Chemistry, University of Alberta, Edmonton, Alberta, Canada, T6G 2G2, and the Structure Determination Laboratory, Department of Chemistry, University of Alberta, Edmonton, Alberta, Canada, T6G 2G2. *Received April 19, 1985*

Abstract: As biomimetic models for the cysteine proteases, four imidazole–thiol pairs, 4(5)-(mercaptomethyl)imidazole (**1a**), 2-(mercaptomethyl)imidazole (**2a**), 2-(mercaptomethyl)-*N*-methylimidazole (**3a**), and 2-(4,5-dimethylimidazol-2-yl)benzenethiol (**4a**) are studied as a function of pH as to their propensity to attack *p*-NPA and dinitrophenylacetate (for **4a**). All species (except **1a**) attack through their thiolate forms and show a plateau region at intermediate pH values which is attributable to attack by the thiolate anion of the zwitterionic forms (ImH^+–S^-). **1a** attacks as its thiolate at high pH and through imidazole N at neutrality. Potentiometric and UV–visible spectrophotometric titrations establish quantitatively the microscopic pK_a values from which are derived the fraction of individual species at any pH. General-base assistance of thiol attack on the acylating agent by the proximal imidazole is not required to explain the result. Deacylation of the corresponding thiol esters **1c–4c** is studied as a function of pH, and in all cases, a plateau region from pH 6.5–7 to 8.5–10 is observed. Solvent deuterium isotope effects from 1.88 (**1c**) to 3.75 (**4c**) are observed at neutral pH values. In all cases, the origin of the plateau region stems from a general-base-promoted delivery of H_2O to the thiol ester by the proximal imidazole. Trapping experiments with Ellman's reagent suggest that *S*- → *N*-acyl transfer is not an important process for these systems. The relevance of these findings is discussed in terms of the mechanism of action of the cysteine proteases.

I. Introduction

The cysteine proteases form a large class of enzymes from plant, animal, and bacterial sources,[1,2] the active sites containing both an essential cysteine SH and histidine–imidazole unit.[3] Although the natural function of the plant enzymes is unknown, their robust character and relative ease of isolation make them commercially valuable[4] as proteolytic agents.

While the detailed mechanism of action is uncertain, papain and other cysteine proteases cleave both ester and amide substrates with the intermediacy of an *S*-acyl-enzyme.[1,5] For ester substrates, the deacylation step is predominantly rate-limiting, while for amides the acylation step is.[6]

The possible sequences for papain-mediated hydrolyses are given in a highly stylized fashion in Figure 1. Early work[7] showed that the pH vs. rate profile for acyl-enzyme formation from a typical ester (*N*-benzoyl-L-arginine ethyl ester (BAEE)) or amide (α-*N*-benzoyl-L-arginamide (BAA)) substrate was bell-shaped and dependent on two groups having apparent pK_a values of ~3.9–4.3 and 8.2–8.5. The former value was originally[7b,8] attributed to a carboxylate residue but was later changed to an imidazolium group;[9] the second pK_a was attributed to the Cys-SH. The general scheme for acylation (Figure 1) was then suggested to involve a general-base role for the imidazole in assisting thiol attack.[9]

However, the most recent evidence from spectral and potentiometric titration as well as from solvent isotope effects[1g,10] indicates that in papain, Cys-25 has an unusually low pK_a of 3–4 while that of His-159 is 8.5. It is proposed[10a] that at physiological pH, 90% of the papain exists in a form wherein the active site

[†] Department of Chemistry.
[‡] Structure Determination Laboratory, Department of Chemistry.

(1) (a) Glazer, A. N.; Smith, E. L. In "The Enzymes"; Boyer, P. D., Ed.; Academic Press: New York, 1971, Vol. 3, pp 502–546. (b) Drenth, J.; Jansonius, J. N.; Koekock, R.; Wolthers, B. G. *Ibid.* 1971, Vol. 3, pp 484–499. (c) Liu, T.-Y.; Elliott, S. D. *Ibid.* 1971, Vol. 3, pp 609–647. (d) Mitchell, W. M.; Harrington, W. F. *Ibid.* 1971, Vol. 3, pp 699–719. (e) Brocklehurst, K. *Methods Enzymol.* **1982**, *87c*, 427. (f) Polgar, L.; Halász, P. *Biochem. J.* **1982**, *207*, 1. (g) Drenth, J.; Kalk, K. H.; Swen, H. M. *Biochemistry* **1976**, *15*, 3731.

(2) (a) Wong, R. C.; Liener, I. E. *B.B.R.C.* **1964**, *17*, 470. (b) Husain, S. S.; Lowe, G. *J. Chem. Soc., Chem. Commun.* **1966**, 1387. (c) Baker, E. N. *J. Mol. Biol.* **1977**, *115*, 263; **1980**, *141*, 441. (d) Tsunada, J. N.; Yasunobu, K. T. *J. Biol. Chem.* **1966**, 4610.

(3) (a) Boland, M. J.; Hardman, M. J. *FEBS Lett.* **1972**, *27*, 282. (b) Boland, M. J.; Hardman, M. J. *Eur. J. Biochem.* **1973**, *36*, 575. (c) Hussain, S. S.; Lowe, G. *Biochem. J.* **1968**, *108*, 855.

(4) (a) Levens, S. M.; Gruber, D. K.; Gruber, C.; Lent, R.; Seifter, E. *J. Trauma* **1981**, *21*, 632 (debridement of burns as a pretreatment for skin grafts). (b) Taussig, S. J.; Yokoyama, M. M.; Chinen, A.; Onari, K.; Yamakido, M.; Nishimoto, Y. *Hiroshima J. Med. Sic.*, **1975**, *24*, 185. (c) A well-known Mexican skin tonic consists of rubbing the facial skin with papaya rind to give a "youthful fresh appearance"; Briskin, M.; Briskin, L. S. In "Make Your Own Cosmetics"; Dell Publishing Co.: New York, 1971; p 63. (d) Commercial meat tenderizing agents list papin (papain) as their active ingredient.

(5) (a) Wilson, I. B.; Bergmann, F.; Nachmansohn, D. *J. Biol. Chem.* **1950**, *186*, 781. (b) Weisz, J. *Chem. Ind. (London)* **1937**, *15*, 685. (c) Lowe, G.; Williams, A. *Biochem. J.* **1965**, *96*, 189. (d) Storer, A. C.; Murphy, W. F.; Carey, P. R. *J. Biol. Chem.* **1979**, *254*, 3163. (e) Brocklehurst, K.; Cook, E. M.; Wharton, C. W. *J. Chem. Soc., Chem. Commun.* **1967**, 1185. (f) Brubacker, L. J.; Bender, M. C. *J. Am. Chem. Soc.* **1964**, *86*, 5333. (g) Smolarski, M. *Isr. J. Chem.* **1974**, *12*, 615. (h) Malthouse, J. P. G.; Gamcsik, M. P.; Boyd, A. S. F.; Mackenzie, N. E.; Scott, A. I. *J. Am. Chem. Soc.* **1982**, *104*, 6811. (i) Lowe, G. *Tetrahedron* **1976**, *32*, 291.

0002-7863/85/1507-7669$01.50/0

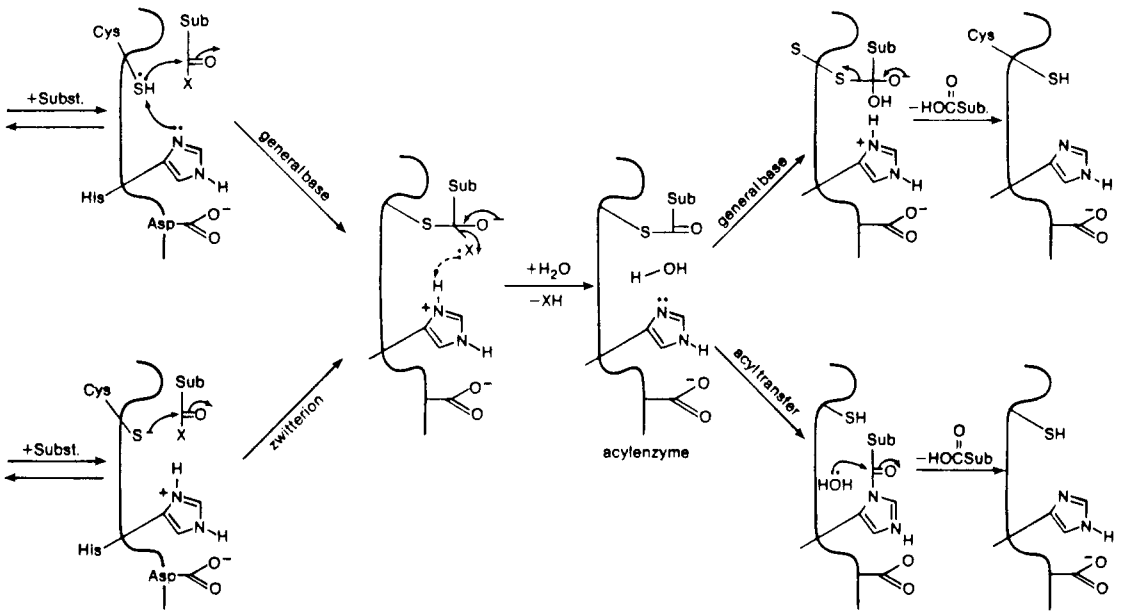

Figure 1. Highly stylized representation of the pathway for ester and amide hydrolyses mediated by papain.

consists of a kinetically competent[10,11] imidazolium–thiolate zwitterionic pair.

The acyl-enzyme, once formed, is hydrolyzed with the assistance of an active site residue having an apparent pK_a of 3.3–4.7, depending upon the substrate.[1a,7a] Also associated with the deacylation step is a D_2O solvent kinetic isotope effect which ranges from 2.75 in the case of α-*N*-benzoyl-L-arginylpapain[7a] to 3.35 for *N-trans*-cinnamoylpapain.[12] This and the fact that the apparent pK_a for deacylation of *trans*-cinnamoylpapain shifts from 4.65 in H_2O to 4.15 in 20% dioxane–H_2O[9b,13d] is consistent with a general-base role for an imidazole unit located in a hydrophobic[5i,13] environment. However, the data do not require a general-base role for the imidazole and could be accommodated by a nucleophilic pathway whereby acyl transfer occurs from the thiol ester to the histidine–imidazole unit with subsequent hydrolysis.[14]

A number of small molecules incorporating both imidazole and a thiol have been investigated as models for the acylation step of papain with esters[14c,15,16] but for the most part showed no cooperative effect of an imidazole unit in the acylation of a thiol such as is believed to occur in the cysteine proteases. Additionally, several imidazole-containing thiol esters have been investigated[14a-c] in an effort to ascertain the role of the intramolecular imidazole in facilitating the breakdown of the normally hydrolysis-resistant[14,17] thiol ester. In these studies, only S → *N*-acyl transfer was observed. No evidence was obtained which would support a general-base role for the imidazole unit although such is believed to be the case in the deacylation of papain.[5i,7a,9b,13]

Recently we reported[18] two studies aimed at providing biomimetic models for both the acylation and deacylation steps in papain-mediated hydrolysis. In the preliminary communication,[18a] (mercaptomethyl)imidazoles **1a–3a** were studied as to their propensity to nucleophilically attack *p*-nitrophenylacetate (*p*-NPA) as a function of pH.

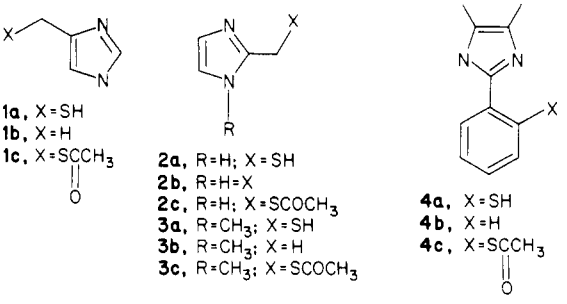

In the second report,[18b] the hydrolysis of thiol ester **4c** was studied as a function of pH and compared with that of **5** and **6**. Herein we report an extension of these studies. As models for

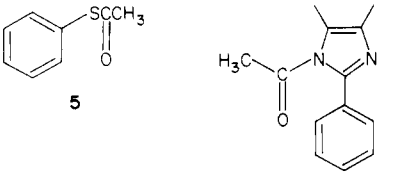

(6) Stevens, F. C.; Glazer, A. N.; Smith, E. L. *J. Biol. Chem.* **1967**, *242*, 2764.

(7) (a) Whitaker, J. R.; Bender, M. L. *J. Am. Chem. Soc.* **1965**, *87*, 2728. (b) Smith, E. L.; Parker, M. J. *J. Biol. Chem.* **1958**, *233*, 1387.

(8) (a) Bernhard, S. A.; Gutfreund, H. *Biochem. J.* **1956**, *63*, 61. (b) Hammond, B. R.; Bernhard, S. A. *Ibid.* **1959**, *72*, 349.

(9) (a) Lucas, E. C.; Williams, A. *Biochemistry* **1969**, *8*, 5125. (b) Lowe, G. *Phil. Trans. R. Soc. London, Ser. B* **1970**, *B257*, 237.

(10) (a) Lewis, S. D.; Johnson, F. A.; Shafer, J. A. *Biochemistry* **1976**, *15*, 5009. (b) *Ibid.*, **1981**, *20*, 48. (c) Johnson, F. A.; Lewis, S. D.; Shafer, J. A. *Ibid.* **1981**, *20*, 52. (d) Sluyterman, L. A. A. E.; Wijdenes, J. *Eur. J. Biochem.* **1976**, *71*, 383. (e) Creighton, D. J.; Schamp, D. J. *FEBS Lett.* **1980**, *110*, 313. (f) Creighton, D. J.; Gessourown, M. S.; Heapeo, J. M. *Ibid.* **1980**, *110*, 319. (g) Polgar, L. *FEBS Lett.* **1974**, *38*, 187; **1974**, *47*, 15. (h) Polgar, L. *Eur. J. Biochem.* **1976**, *71*, 563, 571. (i) Shipton, M.; Kirstan, M. P. J.; Malthouse, J. P. G.; Stuchbury, T.; Brocklehurst, K. *FEBS Lett.* **1975**, *50*, 365.

(11) (a) Angelides, K. J.; Fink, A. L. *Biochemistry* **1978**, *78*, 2659. (b) *Ibid.* **1979**, *18*, 2355.

(12) Brubacher, L. J.; Bender, M. L. *J. Am. Chem. Soc.* **1966**, *88*, 5871.

(13) (a) Johnson, F. A.; Lewis, S. D.; Shafer, J. A. *Biochemistry* **1981**, *20*, 44. (b) Lowe, G.; Whitworth, A. S. *Biochem. J.* **1974**, *141*, 503. (c) Sluyterman, L. A. A. E.; De Graaf, M. J. M. *Biochem. Biophys. Acta* **1972**, *258*, 554. (d) Hinkle and Kirsch (Hinkle, P. M.; Kirsch, J. M. *Biochemistry* **1970**, *9*, 4633) have also reported that the deacylation of furylacryloylpapain depends upon a basic form of the enzyme with pK_a 4.63 (H_2O) and 3.91 (30% dioxane/H_2O) and is independent of pH between 6 and 9. (e) Szawelski, R. J.; Wharton, G. W. *Biochem. J.* **1981**, *199*, 681–697.

(14) (a) Fife, T. H.; DeMark, B. R. *J. Am. Chem. Soc.* **1979**, *101*, 7379. (b) Bruice, T. C. *Ibid.* **1959**, *81*, 5444. (c) Heller, M. J.; Walder, J. A.; Klotz, I. M. *Ibid.* **1977**, *99*, 2780. (d) Bruice, T. C.; Fedor, L. R. *Ibid.* **1964**, *86*, 4880. (e) *Ibid.* **1964**, *86*, 4117. (f) Bender, M. L.; Turnquist, B. W. *Ibid.* **1957**, *79*, 1656. (g) Noda, L. H.; Kuby, S. A.; Lardy, H. A. *Ibid.* **1953**, *75*, 913. (h) Lowe, G.; Williams, A. *Biochem. J.* **1965**, *96*, 194.

(15) (a) Schneider, F.; Wenck, H. *Z. Physiol. Chem.* **1969**, *350*, 1653, 1521. (b) Schneider, F.; Schaich, E.; Wenck, H. *Ibid.* **1968**, *349*, 1526. (c) Petz, D.; Schneider, F. *Z. Naturforsch, C* **1976**, *31C*, 534. (d) Schneider, F. *Z. Physiol. Chem.* **1967**, *348*, 1034.

(16) Lochon, P.; Schoenleber, J. *Tetrahedron* **1976**, *52*, 3023.

(17) (a) Schonbaum, G. R.; Bender, M. L. *J. Am. Chem. Soc.* **1960**, *82*, 1900. (b) Rydlander, P. N.; Tarbell, D. S. *Ibid.* **1950**, *72*, 3021. (c) Morse, B. K.; Tarbell, D. S. *Ibid.* **1952**, *74*, 416.

(18) (a) Skorey, K. I.; Brown, R. S. *J. Am. Chem. Soc.* **1985**, *107*, 4070. (b) Street, J. P.; Brown, R. S. *Ibid.* **1985**, *107*, 6084.

the acylation step, the reaction depicted in eq 1 is studied as a function of pH to determine a profile for the second-order rate constants for **1a–4a** as a function of pH. In addition, we will

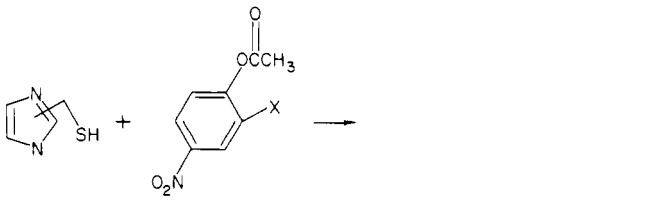

1a-3a, X=H
4a, X=NO_2

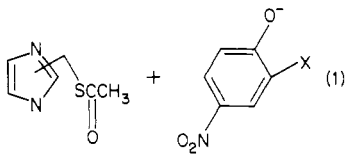

1c-4c (1)

present a full analysis of the microscopic species present in solution in order to determine which is the nucleophilic component at a given pH.

In the subsequent section, we will deal with the hydrolysis of thiol esters **1c–4c** as a function of pH and present a detailed analysis of the kinetics in order to demonstrate that the main pathway at physiological pH for all species involves a general-base delivery of H_2O to the thiol ester by the proximal imidazole.

II. Experimental Section

a. Synthesis. Routine IR, ^1H NMR, and mass spectra were recorded on a Nicolet 7199-FTIR spectrophotometer, a Bruker WP-80 (80 M Hz) NMR spectrometer, and an AEI MS-50 mass spectrometer, respectively. D_2O, Me_2SO-d_6, and MeOH-d_4 (Merck, Sharp & Dohme, Canada) were 99.7% isotopically pure.

2-(2-Mercaptophenyl)-4,5-dimethylimidazole (**4a**) and the corresponding thiol ester **4c** were prepared as reported.[18b]

4(5)-(Mercaptomethyl)imidazole (**1a**), 2-(mercaptomethyl)imidazole (**2a**), and *N*-methyl-2-(mercaptomethyl)imidazole (**3a**) were prepared via a route whereby the corresponding alkyl chlorides[19] (**1–3**; X = Cl) were displaced by benzylmercaptan according to the following general method. To a solution consisting 100 mL of 1.3 N $NaOCH_3$ in dry methanol, 70 mL of dry ethanol, and 2.0 equiv of benzylmercaptan held at reflux was added 0.06–0.10 mol of (chloromethyl)imidazole hydrochloride in 70 mL of dry ethanol. After heating at reflux for 16–20 h, the solution was acidified (pH 1) with 20% ethanolic HCl, and the salts were removed by filtration. The solvent volume was reduced to 60 mL under vacuum and 120–150 mL of H_2O added. Excess benzylmercaptan was extracted with ether and the remaining H_2O layer evaporated under vacuum to dryness. If possible, the remaining oil was recrystallized from ethanol–ether.

4(5)-[(Benzylmercapto)methyl]imidazole–HCl: 61–68% yield; mp 138–143 °C [lit.[20] mp 143–144 °C]; ^1H NMR (MeOH-d_4) δ 8.80 (s, 1 H), 7.55 (s, 6 H), 3.78 (s, 4 H); IR ($CHCl_3$) 3087, 2964, 2616, 2588, 702 cm^{-1}; mass spectrum, *m/z* (rel intensity) 204 (M^+, 9), 113 (3), 91 (28), 82 (100), 81 (74); exact mass calcd for $C_{11}H_{12}H_2S$ 204.0722, obsd 204.0720.

2-[(Benzylmercapto)methyl]imidazole–HCl: 96% (oil); ^1H NMR (MeOH-d_4) δ 7.30 (s, 2 H), 7.25 (s, 5 H), 4.0 (s, 2 H), 3.85 (s, 2 H); IR ($CHCl_3$) 3039, 2822, 2687, 2550, 1610, 765, 704 cm^{-1}; mass spectrum, *m/z* (rel intensity) 204 (M^+, 0.2) 91 (22), 82 (100); exact mass calcd for $C_{11}H_{12}N_2S$ 204.0722, obsd 204.0707.

***N*-Methyl-2-[(benzylmercapto)methyl]imidazole–HCl**: 46% yield; mp 155–157 °C; ^1H NMR (MeOH-d_4) δ 7.25 (m, 7 H), 4.10 (s, 2 H), 3.90 (s, 2 H), 3.75 (s, 3 H); IR ($CHCl_3$) 3120, 2897, 2650, 1597, 1287, 712, 703 cm^{-1}; mass spectrum, *m/z* (rel intensity) 96 (100%), 95 (37%); exact mass calcd for $C_{12}H_{14}N_2S$ 218.0879, obsd 218.0887.

The *S*-benzyl derivatives were converted to the free thiol by the following general procedure.

To a 1-L three-necked flask equipped with a dry ice condensor, magnetic stir bar, and N_2 inlet tube was added 0.025 mol of [(benzylmercapto)methyl]imidazole–HCl and 300 mL of liquid ammonia. To this mixture was added in small portions 3 equiv of Na metal until a blue color persisted. The reaction mixture was stirred for 30–40 min, quenched by the addition of solid NH_4Cl, and liquid NH_3 allowed to evaporate under a stream of N_2 gas. The solid residue was dissolved in 200 mL of dry ethanol and acidified by the addition of 120 mL of 20% ethanolic HCl. The mixture was filtered and then concentrated under vacuum to 30 mL. After final filtration and solvent evaporation to dryness, the remaining solid was recrystallized 2–3 times from deoxygenated ethanolic HCl.

4(5)-(Mercaptomethyl)imidazole–HCl (1a·HCl): 51% yield; mp 119–121 °C [lit.[15d] mp 119–120 °C); ^1H NMR (Me_2SO-d_6) δ 12.0 (br, 2 H), 9.04 (d, 1 H), 7.48 (d, 1 H), 3.80 (d, 2 H), 3.54 (t, 1 H); IR (KBr pellet) 3830, 3106, 2597, 2352, 1614, 821, 622 cm^{-1}; mass spectrum, *m/z* (rel intensity) 114 (M^+, 59), 81 (100); exact mass calcd for $C_4H_6N_2S$ 114.0253, obsd 114.0252. Anal. Calcd for $C_4H_6N_2S$·HCl: C, 32.00; H, 4.70; N, 18.67; S, 21.31; Cl, 23.31. Found: C, 31.73; H, 4.72; N, 18.41; S, 21.56; Cl, 23.27. I_2 titration 99.3 ± 0.5%.

2-(Mercaptomethyl)imidazole–HCl (2a·HCl): 60% yield; mp 77–85 °C (unable to recrystallize satisfactorily due to oxidation to disulfide); ^1H NMR (Me_2SO-d_6) δ 7.55 (s, 2 H), 4.0 (br, 3 H); IR (KBr pellet 3481, 3125, 1611, 1115, 1080, 916, 859, 761, cm^{-1}; mass spectrum, *m/z* (rel intensity) 114 (M^+, 100), 81 (98), 69 (16), 54 (37); exact mass calcd for $C_4H_6N_2S$ 114.0253, obsd 114.0250. I_2 titration 80–85% (20–15% disulfide).

***N*-Methyl-2-(mercaptomethyl)imidazole–HCl (3a·HCl)**: 59% yield; mp 114–118 °C; ^1H NMR (Me_2SO-d_6) δ 7.6 (m, 2 H), 4.1 (s, 2 H), 3.80 (s, 4 H); IR (KBr pellet) 3425, 3152, 1589, 1298, 1101, 782, 642 cm^{-1}; mass spectrum, *m/z* (rel intensity) 128 (M^+, 100), 97 (79), 83 (18); exact mass calcd for $C_5H_8N_2S$ 128.049, found 128.049. Anal. Calcd for $C_5H_8N_2S$·HCl: C, 36.58; H, 5.53; N, 17.08; S, 19.49; Cl, 21.32. Found: C, 36.18; H, 5.51; N, 16.99; S, 19.2; C, 21.2. I_2 titration 98.6 ± 0.5%.

The thiol esters **1c**, **2c**, and **3c** were prepared by the following general method.

To 50 mg of the (mercaptomethyl)imidazole–HCl salt was added 1.5 mL of freshly distilled acetic anhydride. The mixture was heated to attain a clear solution and then allowed to cool. The excess acetic anhydride was removed from the solid residue under vacuum and the remaining material recrystallized from ethanol–ether or 2-propanol–ether to give white crystals.

4(5)-[(Acetylthio)methyl]imidazole–HCl (1c·HCl): 80–90% yield; mp 130–131 °C [lit.[15d] mp 130–133 °C]; ^1H NMR (MeOH-d_4) δ 8.80 (s, 1 H), 7.45 (s, 1 H), 4.25 (s, 2 H), 2.45 (s, 3 H); IR (KBr pellet) 1691.6 cm^{-1}; mass spectrum, *m/z* (rel intensity) 113 (30), 81 (100); exact mass calcd for $C_6H_8N_2OS$ 156.0358, obsd 156.0359. Anal. Calcd for $C_6H_8N_2OS$·HCl: C, 37.40; H, 4.72; N, 14.58; S, 16.67; Found: C, 37.25; H, 4.72; N, 14.56; S, 16.60.

2-[(Acetylthio)methyl]imidazole–HCl (2c·HCl): 80–90% yield; mp 155–159 °C; ^1H NMR (MeOH-d_4) δ 7.60 (s, 2 H), 4.50 (s, 2 H), 2.50 (s, 3 H); IR ($CHCl_3$) 1697.9 cm^{-1}; mass spectrum, *m/z* (rel intensity) 157 (M^+, 2), 114 (40), 113 (88), 81 (100); exact mass calcd for $C_6H_8N_2OS$ 156.0358, obsd 156.0358. Anal. Calcd for $C_6H_8N_2OS$·HCl: C, 37.40; H, 4.72; N, 14.58; S, 16.67; Found: C, 37.47; H, 4.72; N, 14.57; S, 16.58.

***N*-Methyl-2-[(acetylthio)methyl]imidazole–HCl (3c·HCl)**: 80–90% yield; mp 143–144 °C; ^1H NMR (MeOH-d_4) δ 7.50 (m, 2 H), 4.50 (s, 2 H), 3.90 (s, 3 H), 2.40 (s, 3 H); IR (MeOH cast) 1696.6 cm^{-1}; mass spectrum, *m/z* (rel intensity) 170 (M^+, 17), 127 (100), 95 (91); exact mass calcd for $C_7H_{10}N_2OS$ 170.0515, found 170.0513. Anal. Calcd for $C_7H_{10}N_2OS$·HCl: C, 40.77; H, 5.34; N, 13.59; S, 15.53. Found: C, 40.35; H, 5.37; N, 13.59; S, 15.57.

b. Kinetics. (i) Acylation. Buffer materials (sodium acetate (pH 5.0–5.3), succinic acid (pH 5.6–6.5), disodium phosphate (pH 6.7–7.7), boric acid (pH 8.0–9.5), sodium carbonate (pH 9.7–11.0), imidazole, and *N*-methylimidazole) were all reagent grade. Water was triply glass distilled. Ethanol (95%) was used as supplied. *p*-Nitrophenylacetate (*p*-NPA) and 2,4-dinitrophenylacetate (DNPA) were recrystallized from Skelly B and ethyl acetate, respectively.

Kinetics of acylation of **1a–3a** by *p*-NPA were followed at 37.6 ± 0.3 °C by observing the rate of production of *p*-nitrophenoxide at 400 nm under pseudo-first-order conditions of excess **1a–3a** with a Cary 210 UV–visible spectrophotometer interfaced as previously described.[21] All buffers (0.1 M, μ = 0.3 M KCl, H_2O) were carefully deoxygenated by bubbling Ar through the solutions for 4–16 h. Then 3.0 mL of buffer was transferred by syringe to an Ar-flushed, septum-sealed 1.0-cm quartz cell and allowed to equilibrate for 20 min prior to initiation of a run. Varying concentrations of **1a–3a** were then introduced by injection of

(19) Turner, R. A.; Haebner, C. F.; Scholtz, C. R. *J. Am. Chem. Soc.* **1949**, *71*, 2801.

(20) Kelley, J. L.; McLean, E. W.; Miller, C. A. *J. Pharm. Sci.* **1981**, *70*, 341.

(21) Brown, R. S.; Ulan, J. G. *J. Am. Chem. Soc.* **1983**, *105*, 2382.

small aliquots of deoxygenated 0.1 N HCl stock solutions containing 0.1–0.2 M **1a**, **2a**, or **3a**. Runs were initiated by final injection of 5 μL of a 2.6×10^{-2} M *p*-NPA stock solution (ethanol). For the acylation studies, the concentration of **1a–3a** was kept in 10–100-fold excess over that of *p*-NPA. Control experiments using the corresponding imidazoles (**1b–3b**) were conducted in exactly the same manner. Buffer catalysis was not observed from 0.05 to 0.3 M (borate).

The acylation of **4a** by *p*-NPA or DNPA was carried out in an analogous fashion except that in this case, for reasons of solubility, 33 wt % ethanol–H_2O buffers were used. The buffering agents were 0.1 M citrate, acetate, succinate, phosphate, borate, or carbonate, and the pH of the medium was determined by subtracting 0.09 units from the meter reading according to the procedure of Bates et al.[22c] From pH 3.0–6.0 (citrate and acetate buffers), acylation of **4a** was studied by observing the rate of appearance of 2,4-dinitrophenoxide at 400 nm. In a typical run, 3.0 mL of buffer (deoxygenated as above) was placed in a thermostated cuvette along with varying concentrations of **4a**·HCl (prepared as a 0.14 M stock solution in deoxygenated ethylene glycol containing 0.01 M HCl).

DNPA was introduced (3–5 μL of 5.9×10^{-2} M in CH_3CN) to yield a final concentration which was ≤0.1-fold of that of **4a**. Reactions were observed until 70–100% completion and in all cases exhibited excellent pseudo-first-order kinetics. pH was measured by using separate glass and saturated calomel electrodes (Fischer) and a Fischer Model 825 MP meter. No deviation larger than ±0.03 units was detected when comparison of pH before and at the completion of a run was made. In all cases at least duplicate runs were made, the average being taken as k_{obsd}. Buffer catalysis of the second-order rate constants was not observed from 0.02 to 0.1 M.

Second-order rate constants for acylation (k_{cat}^{obsd}) were obtained from the slopes of plots of the pseudo-first-order rate constants (k_{obsd}) for appearance of phenoxide against the concentration of **1a,b**, **2a,b**, **3a,b**, or **4a**. The exact concentration was determined by I_2 titration of the same stock solution of thiol as was used for the kinetics and is typified by the following method for **4a**.

A 5.28×10^{-3} M I_2 solution in 95% ethanol was used as a titrant. Stock **4a** solution (50 μL, 0.14 M in ethylene glycol containing 0.01 N HCl) was injected into 1.0 mL of 95% ethanol containing 10% concentrated HCl. The end point for titration is determined by the persistence of I_2 color.

(ii) Deacylation. Deacylation kinetics for **4c** were carried out in H_2O as described.[18b] Deacylation of **1b**, **2b**, and **3b** was monitored at 260 nm (corresponds to production of thiolate anion) in carefully deoxygenated aqueous buffers, the concentrations of acylated material being between 3×10^{-4} and 3×10^{-3} M. Reactions were generally followed to at least two half-lives and in some cases to completion and exhibited excellent first-order behavior. Rate constants were obtained by fitting the absorbance vs. time data to a standard exponential model,[21] the averages of at least duplicate runs being used to obtain k_{obsd}. Buffer catalysis of the deacylation was not observed between 0.05 and 0.3 M. D_2O kinetic solvent isotope effects for **4c** were monitored as described.[18b] For **1c–3c**, matching 0.1 M, μ = 0.3 M KCl, carbonate buffers were prepared in H_2O and 99.7% D_2O. pD was determined by adding 0.4 units to the meter reading. The pH (pD) values were 10.0 and 10.1, respectively.

(iii) Ellman's Reagent Trapping Experiments. To monitor the total rate of formation of thiolate during the course of deacylation of **2c–4c**, in order to evaluate the S → *N*-acyl equilibrium constant, (K_{eq}, Scheme III), a trapping experiment similar to that employed by Heller et al.[14c] was performed. Varying concentrations of Ellman's reagent (5,5′-dithiobis(2-nitrobenzoic acid)) (DTNB) were placed in the deacylation mixtures and the rate of formation of the dianion of 5-mercapto-2-nitrobenzoic acid was monitored at 412 nm under pseudo-first-order conditions. The usual care concerning deoxygenation of the buffers was employed.

c. Titrations. UV–visible spectrophotometric titrations of **4a** were determined by using a Hewlett-Packard 8450 A Diode Array Spectrophotometer with a built-in 89100A Micro processor. A specially designed cell with a 1.0-cm quartz cuvette attached to an upper reservoir capable of holding 90 mL of solution and having four ports to accommodate pH electrodes, Ar bubbler, and syringe additions was used. To the cell (room temperature) was added 1.0–1.5 mg of solid **4a**·HCl and then 80 mL of deoxygenated 33% ethanol–H_2O solution containing enough HCl to bring the pH to 2–3. The solution was equilibrated with constant Ar bubbling for 5 min, pH was recorded, and then a spectrum from 200–400 nm was taken. Addition of a small aliquot of 0.1 N deoxygenated NaOH to produce a pH increment of 0.2–0.5 units and repeating the equilibration and recording procedure were continued until a final pH of 11 was obtained. In order to check for reversible behavior in the titration, concentrated HCl was added to acidify the solution; the spectrum obtained matched closely the one taken initially at that pH.

Potentiometric titrations of the various species were carried out under carefully deoxygenated conditions in a jacketed cell. The procedure and instrumental set up was closely analogous to that employed before.[22a] Analysis of the pH vs. volume of NaOH-added data by a computer version of Simms' method[22b] yielded the pK_a values. Values given in the tables are averages of duplicate runs.

d. Product Studies. DNPA (13.5 mg) and neutral **4a** (12.0 mg) were placed in an NMR tube, capped with a rubber septum, and flushed with Ar. To this was added 1.0 mL of deoxygenated MeOH-d_4. The ^1H NMR spectrum was monitored, and after $^1/_2$ h, no DNPA was observed, **4c** being produced at the expense of **4a** and DNPA. Repeated monitoring of the spectrum indicated that **4c** solvolyses to yield **4a** and CD_3OCOCH_3, the latter having a sharp singlet at δ 2.03 produced at the expense of the δ 2.33 singlet attributable to the $SCOCH_3$ unit in **4c**.

Similar experiments were conducted with 0.034 M **1a**-, **2a**-, or **3a**·HCl in MeOH-d_4 containing equimolar *p*-NPA. After a 24-h period, 10, 10, and 18% of **1c**, **2c**, and **3c** were detected, the amounts being judged from the intensities of the $SCOCH_3$ singlets. A set of NMR experiments was also conducted wherein the HCl salts of **1a–3a** were neutralized with equimolar trimethylamine prior to reaction with equimolar *p*-NPA in MeOH-d_4. After 24 h, no **1c** was produced from **1a** even though *p*-NPA was ~60% solvolyzed to produce $CH_3CO_2CD_3$ (δ 2.05). However, after 24 h, **2a** and **3a** were completely converted to **2c** and **3c**, respectively, as was evidenced by appearance of the $SCOCH_3$ singlet at δ ~2.4. It is important to note that under these conditions, **1c–3c** are resistant to deacylation.

e. X-ray Crystallography of 4a·HCl and 4a. Suitable crystals of **4a**·HCl were grown by placing 0.2 g of crude material in a small, septum-sealed, Ar-flushed flask along with 2 mL of deoxygenated 0.6 N HCl in 95% ethanol. The contents of the flask were gently heated to dissolve

Table I. Summary of Crystallographic Data

	Crystal Parameters	
formula	$C_{11}H_{13}ClN_2S$	$C_{11}H_{12}N_2S$
fw	240.76	204.30
space group	*C2/c*	*Pbca*
a, Å	20.802 (5)	12.342 (9)
b, Å	8.010 (2)	19.869 (5)
c, Å	14.497 (3)	8.500 (1)
β	99.34 (2)	
C, Å^3	2384	2084
Z	8	8
D_{calcd}, g cm^{-3}	1.342	1.302
μ, cm^{-1}	4.56	2.59
no. and 2θ range for reflcns used in cell detrm	20, 10–32	17, 4–20
crystal dimen, mm	0.19 × 0.15 × 0.44	0.18 × 0.40 × 0.07
	Data Collection and Structure Refinement	
diffractometer	Enraf-Nonius CAD4	Enraf-Nonius CAD4
radiation	Mo Kα (0.71073 Å)	Mo Kα (0.71073 Å)
monochromator	incident beam, graphite cryst	incident beam, graphite cryst
temp, °C	23	23
takeoff angle	3.0°	3.0°
detector aperture	2.40 horiz. × 4.0 vert., mm	2.40 horiz. × 4.0 vert., mm
cryst–detector dist	205 mm	205 mm
scan type	ω–2θ	ω–2θ
scan rate, deg min^{-1}	1.5–10.1	1.1–5.0
scan width, deg in ω	0.80 ± 0.35 tan θ	0.60 + 0.35 tan θ
index range; 2θ limit	*h*,*k*,±*l*; 52.00	*h*,*k*,*l*; 50.00
reflcns measrd	2322 unique $1564I > 3.0\sigma(I)$	1824 unique k82$I > 3\sigma(I)$
no. of refined params	184	80
R_1[a]	0.050	0.051
R_2[b]	0.064	0.052
GOF[c]	1.95	1.49
largest final shift/esd	0.3	0.3
diff Fourier, highest peak	0.37 (7)	0.24 (6)

[a] $R_1 = \sum||F_o| - |F_c||/\sum|F_o|$. [b] $R_2 = (\sum w(|F_o| - |F_c|)^2/\sum wF_o^2)^{0.5}$. [c] GOF $= [\sum w(|F_o| - |F_c|)^2/(N_o - N_v)]^{0.5}$.

(22) (a) Brown, R. S.; Huguet, J. *Can. J. Chem.* **1980**, *58*, 889. (b) Simms, H. S. *J. Am. Chem. Soc.* **1926**, *48*, 1239. (c) Bates, R. G.; Paabo, M.; Robinson, R. A. *J. Phys. Chem.* **1963**, *67*, 1833.

Table II. Positional ($\times 10^4$) and Thermal ($\times 10^2$) Parameters for **4a**·HCl

atom	x	y	z	U, Å^{2a}
Cl	3941.8 (5)	1204 (1)	1458.1 (7)	5.27 (3)+
S	2959.7 (5)	−5639 (1)	−366.5 (7)	5.15 (3)+
N(1)	4274 (1)	−2458 (3)	1198 (2)	3.63 (8)+
N(2)	4273 (1)	−5123 (3)	1205 (2)	3.56 (8)+
C(1)	3194 (1)	−3764 (4)	1257 (2)	3.40 (9)+
C(2)	2726 (1)	−4629 (4)	615 (2)	3.59 (9)+
C(3)	2082 (2)	−4626 (4)	762 (3)	4.5 (1)+
C(4)	1900 (2)	−3773 (4)	1496 (3)	4.9 (1)+
C(5)	2351 (2)	−2875 (5)	2114 (3)	5.2 (1)+
C(6)	2987 (2)	−2875 (4)	1985 (2)	4.5 (1)+
C(7)	3888 (1)	−3789 (4)	1196 (2)	3.42 (9)+
C(8)	4911 (2)	−2953 (4)	1207 (2)	3.70 (9)+
C(9)	4909 (2)	−4643 (4)	1219 (2)	3.55 (9)+
C(10)	5439 (2)	−1715 (5)	1184 (3)	5.7 (1)+
C(11)	5448 (2)	−5892 (5)	1279 (2)	5.0 (1)+

[a] + indicates an atom refined anisotropically. The equivalent isotropic thermal parameter is given by $U = {}^1/_3(U_{11} + U_{22} + U_{33} + 2U_{23} \cos\alpha + 2U_{13} \cos\beta + 2U_{12} \cos\gamma)$.

Table III. Positional ($\times 10^4$) and Thermal ($\times 10^2$) Parameters for **4a**

atom	x	y	z	U, Å^{2a}
S	8311 (1)	901.3 (9)	165 (2)	4.16 (5)+
N(1)	5176 (4)	247 (2)	2590 (6)	3.4 (1)
N(2)	6528 (4)	0 (2)	1087 (6)	3.3 (1)
C(1)	6530 (5)	1162 (3)	2173 (7)	3.4 (2)
C(2)	7519 (6)	1380 (3)	1483 (7)	3.2 (2)
C(3)	7881 (5)	2030 (3)	1855 (8)	3.9 (2)
C(4)	7335 (5)	2440 (4)	2862 (7)	4.8 (2)
C(5)	6373 (6)	2231 (3)	3546 (8)	4.4 (2)
C(6)	5989 (6)	1596 (3)	3189 (8)	4.4 (2)
C(7)	6096 (5)	494 (3)	1972 (7)	3.4 (2)
C(8)	5049 (6)	−427 (3)	2127 (7)	3.7 (2)
C(9)	5895 (6)	−568 (3)	1196 (8)	3.8 (2)
C(10)	4125 (6)	−846 (3)	2691 (8)	5.3 (3)+
C(11)	6189 (6)	−1206 (3)	369 (9)	5.7 (3)+

[a] + indicates an atom refined anisotropically. The equivalent isotropic thermal parameter is given by $U = {}^1/_3(U_{11} + U_{22} + U_{33} + 2U_{23} \cos\alpha + 2U_{13} \cos\beta + 2U_{12} \cos\gamma)$.

all solids and then set aside to crystallize.

Crystals of **4a** were grown by placing equimolar quantities of **4a**·HCl and $NH_4^+HCO_3^-$ in a septum-sealed Ar-flushed vial. Then 1–1.5 mL of deoxygenated 95% ethanol was introduced and the entire mixture heated to ~70 °C, after which it was left to cool to room temperature for several hours.

The crystallographic data concerning compounds **4a**·HCl and **4a** are summarized in Table I. Both structures were solved by using the direct methods program MULTAN.[23a] Refinement of atomic parameters was carried out by using full-matrix least squares to minimize the function $\sum w(|F_o| - |F_c|)^2$ where w is given by $4F_o^2/\sigma^2(F_o^2)$. All calculations were performed by using the SDP program package.[23b]

In structure **4a**-HCl, a difference Fourier showed an apparent disordering of the position of the H atom on S. No attempt was made to model this disorder, and this atom was not included in the refinement calculations. For **4a**-HCl, there was sufficient data to permit refining all non-H atoms with anisotropic thermal parameters. However, this was not the case for **4a**, and only the S atom and the two methyl C atoms were refined anisotropically. All H atoms were refined in **4a**-HCl. In **4a**, only the two H atoms on N were refined as independent atoms; the remainder were constrained to "ride" with their attached C atom. The thermal parameters for these riding atoms were refined for a few cycles before being fixed in the final cycle.

The positional and thermal parameters for **4a**·HCl and **4a** are given in Tables II and III, respectively.[24]

(23) (a) Main, P.; Lessinger, L.; Woolfson, M. M.; Germain, G.; Declercq, J. P. MULTAN 11/82. A System of Computer Programs for the Automatic Solution of Crystal Structures from X-Ray Diffraction Data. (b) The computer programs used in this analysis include the Enraf-Nonius Structure Determination Package by B. A. Frenz ("Computing in Crystallography"; Delft University Press: Delft, Holland, 1978; pp 64–71) and several locally written or modified programs.

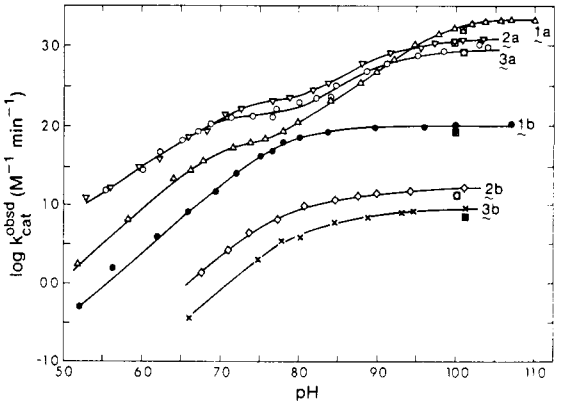

Figure 2. Plot of the log second-order rate constant vs. pH profile for attack of **1a–3a** and their parent imidazoles **1b–3b** on *p*-NPA; T = 37.0 °C, 0.1 M aqueous buffers, μ = 0.3 M KCl. Data points enclosed in squares represent D_2O solution. Solid lines through the data for **1a–3a** represent nonlinear least-squares fitting according to eq 2, while those for imidazoles **1b–3b** are fits according to eq 3.

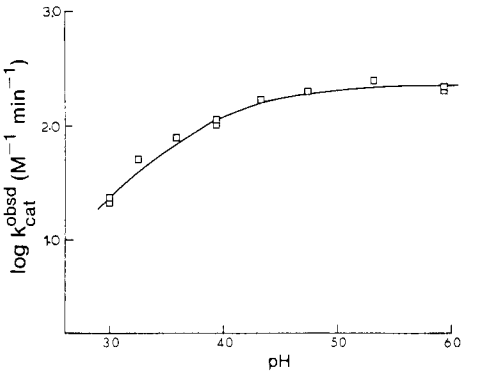

Figure 3. Plot of the log second-order rate constant vs. pH profile for attack of **4a** on DNPA; T = 37.0 °C, 0.1 M buffers, 33% ethanol/H_2O. Solid line represents nonlinear least-squares fit of the data to eq 4.

Scheme I

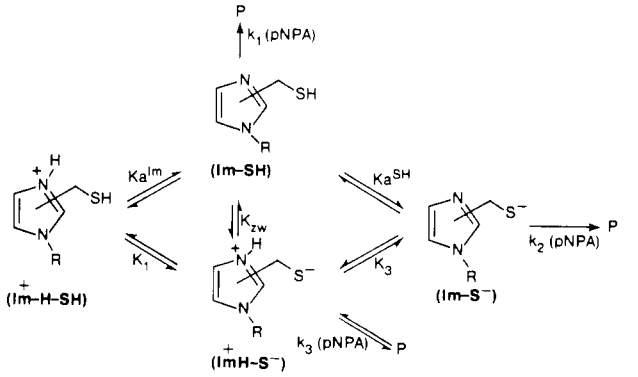

Scheme II

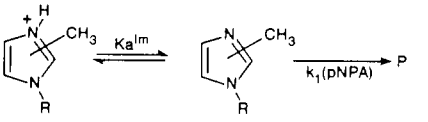

III. Results and Discussion

a. Acylation. Shown in Figures 2 and 3 are the second-order rate constant (k_{cat}^{obsd}) vs. pH profiles for acylation of **1a,b–3a,b** and **4a**, respectively. For the former, the acylating agent was *p*-NPA, while due to the low pH values required to define the kinetic pK_a DNPA was used as an acylating agent for **4a**. In Figure 2, the

(24) Additional tables of data including H coordinates, torsional angles, and structure factors can be found in supplementary data.

Table IV. Potentiometric Titration Macroscopic and Microscopic pK_a Values for **1a,b–4a,b** and Corresponding *S*-Benzyl Derivatives[a]

	macroscopic pK_a[a]		microscopic pK_a[b,c]				K_{zw} =
compd	pK_1	pK_2	pK_1	pK_a^{Im}	pK_3	pK_a^{SH}	K_1/K_a^{Im}
4a[d]	3.9 ± 0.1	9.0 ± 0.1	3.9	7.0	9.0	5.9	1260
4b[d]	7.0 ± 0.1						
4-S-Bz[d]	7.0 ± 0.1						
1a	6.54	9.54	7.72	6.57	8.36	9.51	0.07
2a	6.37	9.26	6.50	6.96	9.13	8.67	2.88
3a	6.31	8.88	6.47	6.83	8.75	8.39	2.29
1b	7.56[e]						
2b	7.94[e]						
3b	7.64[e]						

[a] Determined at 25 °C in H_2O; averages of at least duplicate determinations ±0.05 units unless otherwise specified. [b] pK_a^{Im} assumed to be the same as the corresponding *S*-benzyl derivative.[27] [c] Calculated according to methods given in ref 29. [d] Determined in 33% ethanol–H_2O. [e] Literature values for **1b**, **2b**, and **3b** are 7.51, 8.00, and 7.85, respectively.[30]

solid lines through the data are computer-generated fits to eq 2 and 3. Equation 2 describes the minimum reaction scheme

$$k_{cat}^{obsd} = \frac{(k_1K_a^{Im} + k_3K_a^{Im}K_{zw})[H^+] + k_2K_a^{Im}K_a^{SH}}{[H^+]^2 + (K_a^{Im} + K_a^{Im}K_{zw})[H^+] + K_a^{Im}K_a^{SH}} \quad (2)$$

$$k_{cat}^{obsd} = \frac{k_1K_a^{Im}}{K_a^{Im} + [H^+]} \quad (3)$$

$$k_{cat}^{obsd} = \frac{k_3K_1}{K_1 + [H^+]} \quad (4)$$

involving zwitterions for thiols **1a–3a** (Scheme I), while eq 3 describes the reaction with imidazoles **1b–3b** (Scheme II).

In Figure 3, the solid line represents a computer-generated fit to eq 4 which describes the situation for **4a** as in Scheme I but without involvement of ImSH or ImS^-.

Evaluation of the individual parameters in eq 2 which pertain to the activity of the zwitterions (k_3 and K_{zw}) is not possible unless additional information is available, since the observed data apparently fit the simplified but kinetically equivalent scheme having two pK_a values as in eq 2a. This is easily verified by assuming that in Scheme I, $K_{zw} = [ImH^+—S^-]/[Im\text{-}SH]=O$.

$$k_{cat}^{obsd} = \frac{k_1K_a^{Im}[H^+] + k_2K_a^{Im}K_a^{SH}}{[H^+]^2 + K_a^{Im}[H^+] + K_a^{Im}K_a^{SH}} \quad (2a)$$

The additional information is available from an analysis of the microscopic ionization constants in Scheme I. Given a dibasic acid having two ionizable groups with pK_a values not too widely separated, there are four microscopic ionizations yielding four ionic species in solution. For amphoteric molecules such as amino acids, the pK_a of the carboxylic acid is considerably lowered and pK_a of the ammonium group is considerably raised relative to appropriate comparison species where the groups are isolated.[25] Should such obtain for **1a–4a**, then as the individual pK_a values (of each group ionizing while the other is neutral) approach each other so that $pK_a^{SH} - pK_a^{Im}$ (Scheme I) is roughly 2 or less, large amounts of zwitterionic material will be present at physiological pH.

Consider the situation for **4a**. Potentiometric titration of **4a** in 33% ethanol–H_2O yields two pK_a values (Table IV) of 3.9 ± 0.1 and 9.0 ± 0.1. Shown in Figure 4 are the spectrophotometric changes accompanying the ionizations. The low pK_a is clearly attributable to formation of a benzenethiolate anion as is evidenced by the formation of the long-wavelength band centered at 350–360 nm. Spectrophotometric titration of **4b** having no thiol present gives a spectrophotometric pK_a of 7.0 and no such long-wavelength band. The spectral changes shown in Figure 4b correspond to transition from the zwitterionic to anionic forms. On deprotonation, the long-wavelength band which is predominantly attrib-

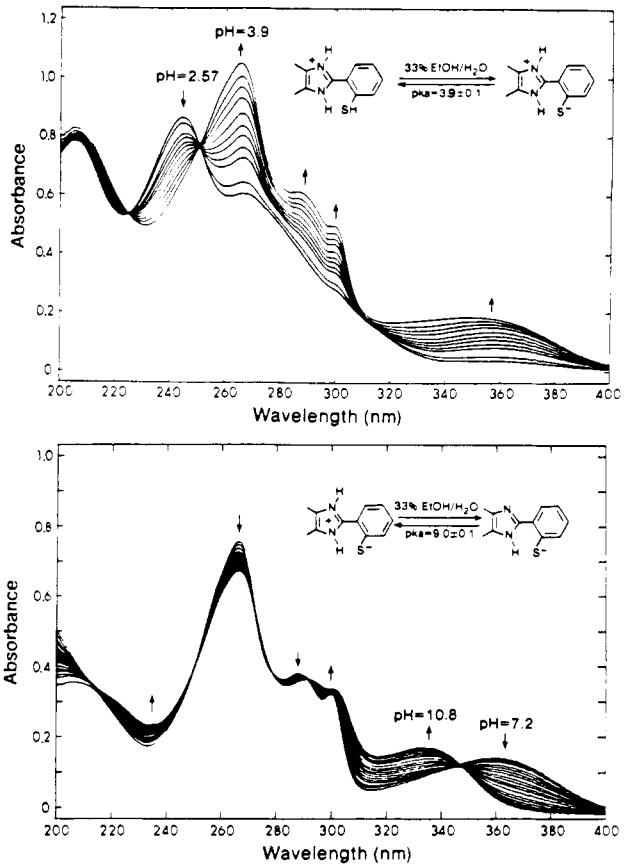

Figure 4. pH vs. UV–visible absorption spectra for 4.6×10^{-5} M **4a** 33% ethanol/H_2O, unbuffered, deoxygenated by Ar-flushing.

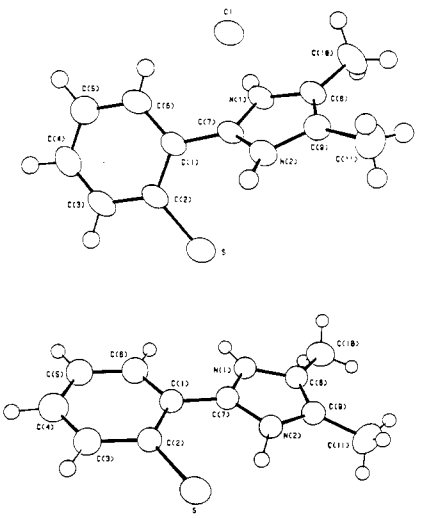

Figure 5. X-ray crystal structures for **4a**·HCl and **4a**. For additional structural data, see supplementary material.

utable to benzenethiolate undergoes a slight hyposochromic shift since the neutral imidazole is poorer at stabilizing the thiolate form than is a positively charged imidazolium ion. Both spectral titrations show tight isosbestic points and are completely reversible provided deoxygenation is complete.

For **4a**, the spectrophotometric pK_a values equal those determined from potentiometric titration. When compared to a variety of benzenethiols which have pK_a values in the range 5.5–6.0,[26] pK_1 of **4a** to form the zwitterion-stabilized form (ImH^+–S^- in Scheme I) is reduced by 1.6–2.1 units. Similarly, the imidazolium pK_a of ImH^+–S^- of **4a** (pK_3, Scheme I) is raised relative to that of **4b** (7.0, Table IV) by some 2.0 units. In this particular system,

(25) See, for example: Loudon, G. M. "Organic Chemistry"; Addison-Wesley Co.: Reading, MA, 1984; pp 1315–1319.

(26) Hupe, D. J.; Jencks, W. P. *J. Am. Chem. Soc.* **1977**, *99*, 451.

Table V. Selected Geometrical Parameters for Salt and Zwitterionic Forms of **4a**

atoms	salt	zwitterion
	Bond Distances	
S–C(2)	1.772 (3)	1.765 (6)
N(1)–C(7)	1.335 (3)	1.345 (7)
N(1)–C(8)	1.381 (3)	1.404 (7)
N(1)–HN(1)	0.79 (3)	0.94 (7)
N(2)–C(7)	1.334 (3)	1.347 (7)
N(2)–C(9)	1.376 (3)	1.376 (7)
N(2)–HN(2)	0.84 (3)	1.17 (7)
C(1)–C(7)	1.460 (3)	1.442 (7)
C(8)–C(9)	1.354 (3)	1.340 (8)
mean phenyl C–C	1.38 (2)	1.39 (2)
	Bond Angles	
C(7)–N(1)–HN(1)	124 (2)	125 (4)
C(8)–N(1)–HN(1)	125 (2)	126 (4)
C(7)–N(2)–HN(2)	121 (2)	114 (3)
C(9)–N(2)–HN(2)	129 (2)	136 (4)
C(2)–C(1)–C(7)	122.3 (2)	123.4 (5)
C(6)–C(1)–C(7)	118.8 (2)	117.7 (6)
S–C(2)–C(1)	120.3 (2)	125.0 (4)
S–C(2)–C(3)	121.3 (2)	117.6 (5)
	Torsion Angle	
N(2)–C(7)–C(1)–C(2)	−57.3	−2.4

it can be demonstrated that the zwitterionic form (ImH^+–S^-) vastly exceeds in concentration the neutral form (Im–SH) at any pH since $K_{zw} = [ImH^+–S^-]/[Im–SH] = K_1/K_a^{Im}$. Since K_a^{Im} for **4a** can be reasonably approximated by the pK_a of the corresponding *S*-benzyl derivative,[27] K_{zw} can be calculated to be 1260.

Crystallographic structures of both the salt and zwitterion forms of **4a** are presented in Figure 5 along with selected geometrical parameters in Table V. The HCl salt, **4a**·HCl, exists in a form wherein the dihedral angle between the two rings is 57.3° and an imidazole N–H unit is H-bonded to the Cl^-. On deprotonation, the two rings become essentially coplanar (dihedral angle = 2.4°). The driving force for this process likely derives from a tight $S^-\cdots H–N(2)^+$ H-bond. In this structure, the $H–N(2)^+$ bond length is 1.17 (7) Å, elongated from the H–N(1) bond length of 0.94 (7) Å and from other typical N–H distances.[28a] The $S^-\cdots H–N(2)^+$ contact distance is 1.94 (7) Å which is considerably longer than an S–H bond distance (1.17–1.37 Å)[28b,c] but well within the sum of the van der Waals radii for the two atoms (3.0 Å). It is quite definite that the material, when neutral, exists completely in a zwitterionic form in the crystal as well as solution phase.

Having established that a thiol pK_a decreases in the presence of a proximal imidazolium ion while that of the imidazolium increases in the presence of a thiolate anion, at least in a specialized system where $pK_a^{SH} < pK_a^{Im}$, it is necessary to demonstrate that the same effect is obtained in other systems where $pK_a^{SH} > pK_a^{Im}$, a more common situation. For imidazole–thiols **1a–3a**, the microscopic pK_a values can easily be calculated[29] from potentiometrically determined macroscopic pK_a values provided that one has an assumed value for one of the microscopic values. In Scheme I, it is reasonable to assume that pK_a^{Im} is roughly equivalent to that of the corresponding *S*-benzyl derivative.[27] Under this assumption, the microscopic pK_a values given in Table IV can be calculated as well as the K_{zw} equilibrium constant. The most important observation is that repositioning the thiolmethyl group from the 4(5)-position to the 2-position has the net effect of both raising pK_a^{Im} and reducing pK_a^{SH}, the latter undoubtedly due to a larger inductive withdrawing effect of the two N's.

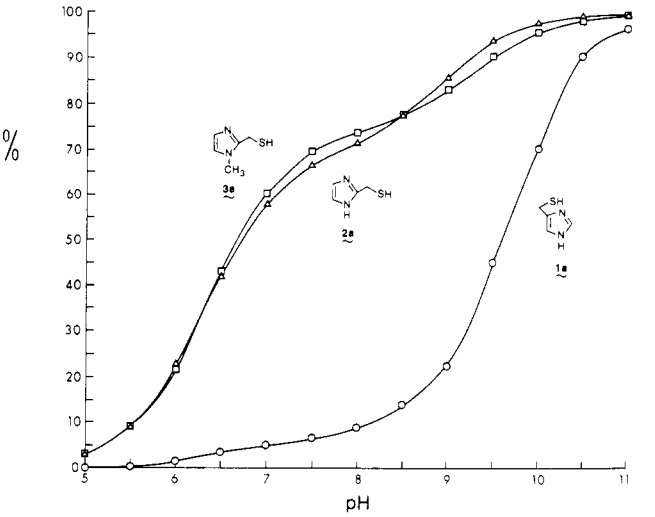

Figure 6. Plot of total [thiolate], i.e., [ImH^+–S^-] + [Im–S^-], as a function of pH for **1a–3a** calculated from the microscopic dissociation constants gives in Table IV.

Given the microscopic pK_a values in Table IV, it is possible to calculate the concentration of each species as a function of pH. For **1a** where $pK_a^{SH} - pK_a^{Im} \simeq 3$, only a small proportion of ImH^+–S^- is present at physiological pH. However, for **2a** and **3a** where $pK_a^{SH} - pK_a^{Im} \simeq 1.7$ and 1.6, the zwitterionic form is the dominant species in solution from pH 6.5 to 9. Finally, shown in Figure 6 is a plot of total thiolate present ([ImH^+–S^-] + [Im–S^-]) as a function of pH. It is apparent that while very little thiolate of any form is present for **1a** at neutral pH, both **2a** and **3a** retain large proportions of thiolate in that region.

Typically, thiols react with esters such as *p*-NPA as their corresponding thiolate anions[17,31] and do not, insofar as we are aware, require general-base assistance if the rate-limiting step is attack.[31,32] It is expected that the thiolate anion of ImH^+–S^- is also capable of acting as a nucleophile toward *p*-NPA, albeit a weaker one than in Im–S^- because the former is a weaker base.[26] For **1a**, the observed plateau in the pH/rate constant profile (Figure 2) is comparable to that exhibited by the parent imidazole, **1b**, and is therefore best explained in terms of a nucleophilic attack on *p*-NPA by the deprotonated imidazole.[33] (In Figure 2, the filled square symbols at ~pH 10 are points derived from D_2O solution; $k_{H_2O}/k_{D_2O} \simeq 1$). The heterocyclic N of **2b** and **3b** shows a much reduced propensity to act as a nucleophile because the steric encumbrance provided by the 2-CH_3 group toward nucleophilic attack by N cannot be avoided.[33c] Such should also

(27) (a) Wegscheider, R. *Monatsh. Chem.* **1902**, *23*, 287. (b) Ebert, L. *Z. Phys. Chem.* **1926**, *121*, 385. (c) The pK_a value of 5-(methylthiol)glycolic acid at 3.72 is nearly equal to that of the CO_2H unit in thiolglycolic acid at 3.67 which gives some justification to the "equivalence postulate" as applied to SH and SCH_3 groups.[27d] We do not expect that the *S*-benzyl group will markedly alter these conclusions since the σ_m and σ_I values for CH_3 and $CH_2C_6H_5$ are essentially the same.[27e] (d) Brown, H. C.; McDaniel, D. H.; Häfliger, O. In "Determination of Organic Structures by Physical Methods"; Braude, E. A., Nachod, F. C., Eds.; Academic Press: New York, 1955; pp 620, 632. (e) Exner, O. "Correlation Analysis in Chemistry"; Chapman, N. B., Shaster, J., Eds.; Plenum Press: London, 1978.

(28) (a) An examination of 142 compounds from the Cambridge Crystallographic Data Base ave 167 N–H distances with a mean value of 0.91 Å. (b) Krebs, B.; Henkel, G.; Dinglinger, H.-J.; Stehmeier, G. *Z. Krist.* **1980**, *153*, 285. (c) Howard-Lock, H. E.; Lock, C.J. C.; Smelly, P. S. *J. Cryst. Spectrosc.* **1983**, *13*, 333.

(29) For methods of calculation of microscopic pK_a values from macroscopic pK_a data see: (a) Clement, G. E.; Hartz, T. P. *J. Chem. Educ.* **1971**, *48*, 395. (b) Edsall, J. T.; Blanchard, M. H. *J. Am. Chem. Soc.* **1933**, *55*, 2337. (c) Edsall, J. T.; Martin, R. B.; Hollingworth, B. R. *Proc. Natl. Acad. Sci. U.S.A.* **1958**, *44*, 505. (d) Benesch, R. E.; Benesch, R. *J. Am. Chem. Soc.* **1955**, *77*, 5877.

(30) Perrin, D. D. "Dissociation Constants of Organic Bases in Aqueous Solution"; Butterworths: London, 1965.

(31) (a) Lindley, H. *Biochem. J.* **1966**, *74*, 577. (b) Whittaker, J. R. *J. Am. Chem . Soc.* **1960**, *84*, 1900. (c) Ogilvie, J. W.; Tildon, J. T.; Strauch, B. S. *Biochemistry* **1964**, *3*, 754. (d) Fersht, A. R. *J. Am. Chem. Soc.* **1971**, *93*, 3504. (e) Brembilla, A.; Roizard, D.; Schoenleber, J.; Lochon, P. *Can. J. Chem.* **1984**, *62*, 2330.

(32) (a) Lienhard, G. E.; Jencks, W. P. *J. Am. Chem. Soc.* **1966**, *88*, 3982. (b) Barnett, R. E.; Jencks, W. P. *Ibid.* **1967**, *89*, 5963. (c) *Ibid.* **1969**, *91*, 2358.

(33) (a) Bender, M. L.; Turnquist, B. W. *J. Am. Chem. Soc.* **1957**, *79*, 1652. (b) Bender, M. L. *Chem. Rev.* **1960**, *60*, 53. (c) Bender, M. L. "Mechanisms of Homogeneous Catalysis From Protons to Proteins"; Wiley-Interscience: New York, 1971; pp 147–176.

obtain for **2a** and **3a**, but since they are 10–15-fold more active at neutrality than their parent imidazoles, nucleophilic attack by S^- is indicated.

The pH/rate constant profile given in Figure 3 clearly shows a dependence of the nucleophilicity on a basic form of **4a** having a kinetic pK_a of 3.92 ± 0.05, this value being obtained from fitting of the data to eq 4. Since the kinetic, spectrophotometric, and potentiometric titration-derived pK_a values are the same, strong evidence for nucleophilic activity by the zwitterionic form of **4a** is provided.

Throughout the above discussion, we have maintained that **2a**, **3a**, and **4a** attack throughout the pH profile by way of thiolate ions, ImH^+–S^- and Im–S^-. However, at neutrality, **1a** attacks through the imidazole nitrogen because very little of its corresponding ImH^+–S^- form is present. Evidence to support these statements is as follows. Firstly, ^1H NMR spectra of the HCl salts of **1a–3a** and **4a** alone in MeOH-d_4 containing equimolar *p*-NPA or DNPA (for **4a**) show formation of the corresponding thiol ester at the expense of the parent thiol. Under these conditions, **4c** is slowly solvolyzed to regenerate **4a** + CD_3OCOCH_3, but thiol esters **1c–3c** are stable. However, when neutralized, NMR analysis of **1a–3a** + *p*-NPA in MeOH-d_4 indicates that only **2a** and **3a** become S-acylated. With **1a** present, *p*-NPA is solvolyzed to produce $CH_3CO_2CD_3$ without the intervention of **1c**. Thiol ester **1c** was stable under these conditions so that if it were produced from **1** and *p*-NPA, it would have been observed. Secondly, UV–visible experiments on solutions of equimolar **2a** or **3a** and *p*-NPA (4×10^{-4} M, pH 7.8, 0.1 M phosphate, μ = 0.3 M KCl, T = 25 °C) as a function of time follow second-order kinetics, and not pseudo-first-order, for the production of *p*-nitrophenoxide, the second-order rate constants (k_{cat}^{obsd}) being 207 ± 50 M^{-1} min^{-1} and 205 ± 65 M^{-1} min^{-1}, respectively. When allowances are made for the experimental errors, these constants compare favorably with those derived from the graph in Figure 2 (207 and 167 M^{-1} min^{-1}, respectively). However, under the same conditions, the reaction of **1a** + *p*-NPA follows pseudo-first-order kinetics. This is expected if **1a** attacks through imidazole since the corresponding *N*-acylimidazole should hydrolyze rapidly and regenerate **1a**.[33]

Finally, under these conditions, thiol esters **1c–3c** hydrolyze very slowly which supports their involvement in the reaction of **2a** or **3a** (but not **1a**) with *p*-NPA. Hence, these materials are not true turnover catalysts but rather acyl-transfer reagents. On the other hand, **4a** is indeed a turnover catalyst since at neutrality, the thiol ester **4c** hydrolyzes rapidly enough to regenerate the catalyst during the course of the acylation experiment.

Having obtained the necessary microscopic pK_a data (Table IV), it is now possible to return to the quantitative analysis of the pH/rate constant profiles in terms of eq 2–4. Separation of the composite term $K_a^{Im}(k_1 + k_3K_{zw})$ to evaluate k_3, the nucleophilic rate constant for the zwitterionic forms, is made by assuming that k_1 for **1a–3a** roughly is the same as that of the corresponding imidazoles. The derived values are given in Table VI.

Uncertainties in the microscopic pK_a values which are used to calculate K_{zw} cause a ±20% cumulative error in k_3. These are unavoidable since the ±0.05 deviations in the macroscopic pK_a values accumulate in the calculations for the microscopic values.[29] Nevertheless, the nucleophilicity of the thiolate in the zwitterionic form (when compared with that of the anionic ImS^- form) is commensurate with its basicity. Hupe and Jencks[26] have shown that the attack of basic thiolate anions on substituted phenylacetates shows a small dependence on thiol basicity (β_{NUC} = 0.27) and a break near ΔpK_a = 0 to a slope of β_{NUC} = 0.84 as the pK_a of the thiol is decreased and phenolate expulsion becomes rate-limiting. Based on the microscopic pK_a values in Table IV and the known pK_a of 7.13 for *p*-nitrophenol,[26,30] it can be calculated[34] that k_2/k_3 for **2a** should be 8.81, while k_2/k_3 for **3a** is 7.85. The corresponding derived values from Table VI of 6.61 and 8.30 for **2a** and **3a** are remarkably close and once again lend credence to the interpretation that it is the ImH^+–S^- thiolate that is responsible for nucleophilic attack on *p*-NPA in the plateau region.

Table VI. Computed Rate Constants for the Attack Of the Various Ionic Forms of **1–4** on *p*-NPA[a] and **4a** on DNPA[b] at 37 °C in H_2O (**1–3**) and 33% Ethanol–H_2O (**4a**)[c]

compd	k_1, M^{-1} min^{-1}	k_2, M^{-1} min^{-1}	k_3, M^{-1} min^{-1}
1a	*d*	2275	*e*
2a	*d*	1071	162
3a	*d*	1179	142
1b	92.5		
2b	7.64		
3b	13.2		
4a[f]	*g*		4.0
4a[h]	*g*		217

[a] Rate constants as defined in Schemes I and II, values obtained by fitting data to eq 2 (**1a–3a**) and eq (**1b–3b**). [b] Rate constants defined as in Scheme I; obtained by fitting data to eq 4. [c] Cumulative errors resulting from deviations in pK_a values force errors in k_2 and k_3 to be 20% and 5%, respectively, but do not alter conclusions in text. [d] Assumed to be the same as k_1 for corresponding imidazoles. [e] Not determinable. [f] Using *p*-NPA, pH 6.85 (succinate) –7.51 (phosphate). [g] Negligible relative to k_3. [h] Using DNPA, pH region defined in Figure 3.

From pH 6.85 to 7.5, the attack of **4a** on *p*-NPA can be observed and shows a second-order rate constant (k_3) of 4.0 M^{-1} min^{-1}, roughly 50-fold lower than the rate constant for attack on the more activated substrate DNPA. The relatively low value for k_3 with *p*-NPA for **4a** compared with **2a** or **3a** is an expected consequence of the lower basicity of the former,[26] i.e., pK_1 = 3.9.

Finally, we wish to point out that these systems represent the only clear-cut examples wherein an imidazole and thiol unit cooperatively interact in an acyl-transfer reaction. We have presented evidence that the apparent "extra" activity of **1a** at neutrality which had originally been interpreted[15] as arising from an ImH^+–S^- form or general-base catalysis of thiol attack by Im is in reality attributable to nucleophilic involvement of the imidazole. That the zwitterionic form is not prominent in this system is a result of the relatively large disparity between pK_a^{SH} and pK_a^{Im}. Lochon and Schonleber[17] have reported a residual activity at neutrality in the acylation of some 2-(thiomethyl)benzimidazole derivatives and have attributed its origin to a general-base role whereby the benzimidazole ring deprotonates the thiol in assisting the attack on *p*-NPA. The residual activity is quite real in our opinion and cannot be explained on the basis of benzimidazole nucleophilicity.[33c] We feel it is more probable that a nonnegligible zwitterionic component akin to those demonstrated here is responsible. However, more work on that specific system would be required before a clear distinction can be made.

Overberger and co-workers[35] were able to demonstrate only additive rather than cooperative effects between imidazole and thiol in attacking p-NPA with copolymers derived from vinylimidazole and vinylthiol. This is likely a result of the ill-defined proximity of the interacting groups. The same explanation is probably responsible for the lack of cooperativity toward *p*-NPA attack observed for a series of peptides incorporating various arrangements of cysteine and histidine.[14c] The present data suggest that the minimum requirements for cooperativity are a closeness in both pK_a and proximity in order to take advantage of the internal electrostatic stabilization of the zwitterionic form.

b. Deacylation. Earlier studies have shown that thiol esters are not particularly susceptible to nucleophilic attack by oxyanions[14,17,26,32] but are very rapidly attacked by nitrogen-based nucleophiles.[36] Intermolecular general-base-catalyzed hydrolysis

(34) For **2a**, the expected reduction of k_3 relative to k_2 is $10^{(0.27(8.67-7.13)+0.84(7.13-650))} = 8.81$, while for **3a** it is $10^{(0.27(8.39-7.13)+0.84(7.13-6.47))} = 7.85$.

(35) Overberger, C. G.; Pacansky, T. J.; Lee, J.; St. Pierre, T.; Yaroslavsky, S. *J. Polym. Sci. Symp.* **1974**, *46*, 204.

(36) (a) Bruice, T. C. In "Organic Sulfur Compounds"; Kkarasch, N., Ed.; Pergamon Press: New York, 1959; Vol. 1, p 421. (b) Schwyzer, R. *Helv. Chem. Acta* **1953**, *54*, 414. (c) Hawkins, P. J.; Tarbell, D. S. *J. Am. Chem. Soc.* **1953**, *75*, 2982. (d) Wieland, T.; Lang, H. U.; Liebach, O. *Ann.* **1955**, *597*, 227 and references therein. (e) Connors, K. A.; Bender, M. L. *J. Org. Chem.* **1961**, *26*, 2498.

of ethyl trifluorothiolacetate[37] has been observed as have second-order terms of hydroxylamine,[14d] morpholine, and hydrazine[14e] attack on some unactivated thiol esters and δ-thiolvalerolactone. However, *intramolecular* general-base catalysis on unactivated thiol esters has not been observed to our knowledge (with the notable exception of **4c**[18]). Previous studies by Bruice[14b] and Fife and DeMark[14a] have shown that **7** and **8**, respectively, simply undergo rapid nucleophilic S → *N*-acyl transfer. The major

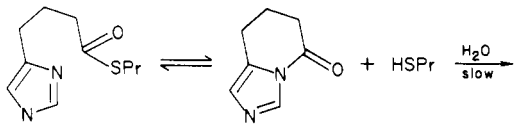

7

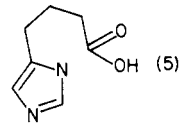

(5)

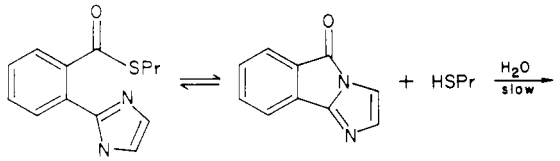

8

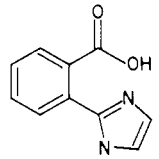

(6)

drawback with respect to comparing these systems to the enzymatic deacylation is that in **7** and **8**, ring closure occurs with the expulsion of the HSR unit, while in the enzyme the imidazole and HS-Cys groups are retained in the active site. Bruice[14b] was aware of this problem and noted that when 0.2 M 2-mercaptoethanol was added to the solution, the hydrolysis of thiol ester **7** was completely inhibited due to a mass action effect (with re-formation of the SCH_2CH_2OH ester). This observation also indicates that in this system, the intramolecular imidazole is incapable of acting as an effective general base in promoting thiol ester decomposition.

Our previous report[18b] indicated that when the imidazole and thiol groups are retained in the same molecule (as in **4c**), the predominant form in solution is the *S*-acyl derivative. Furthermore, the imidazole is capable of acting as a reasonably effective intramolecular general base in promoting the hydrolysis of **4c**. Indeed, the hydrolysis of **4c** from pH 7.0 to 10 is independent of pH and proceeds with a k_{obsd} of 1.4×10^{-3} s^{-1} in H_2O which compares favorably with the reported rate constant for deacylation of *trans*-cinnamoyl papain ($k_{deacyl} = 3.68 \times 10^{-3}$ s^{-1}).[38]

Examination of molecular models of **4c** suggests that there is severe steric compression to the insertion of an H_2O molecule between the imidazole N and S–$COCH_3$ unit as would be required for a general-base pathway. It was originally felt[18b] that the rather slow rate of deacylation of **4c** (when compared to the best deacylations for papain) was due to this nonoptimum fit and might be improved by a suitable structural change as would be accomplished in **1c–3c**.

Shown in Figure 7 are the pH vs. log k_{obsd} profiles for the decomposition of thiol esters **1c–4c** in H_2O as well as the curve reported for *N*-acetylimidazole.[39] The solid lines through the

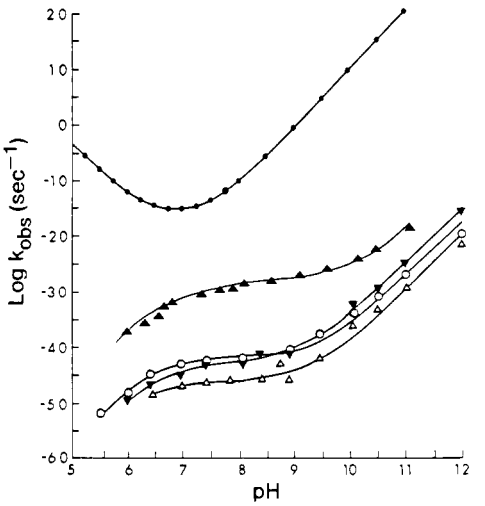

Figure 7. Plot of the pseudo-first-order rate constants for vs. pH for the decomposition of thiol esters **1c–4c** (H_2O, 0.1 M buffers, μ = 0.3 M KCl, T = 37 °C). Solid lines are obtained by nonlinear least-squares fitting of the data to eq 7. Data for *N*-acetylimidazole obtained from ref 39a (●), **1c** (△), **2c** (▼), **3c** (○), **4c** (▲).[18b]

Table VII. Computer-Generated Equilibrium and Rate Constants from Nonlinear Least-Squares Fitting of k_{obsd} vs. pH Data for Hydrolysis of **1c–4c** to Eq 7[a]

compd	k_1(HOH), s^{-1}	k_2, M^{-1} s^{-1}	pK_a^{Im}	k_{H_2O}/k_{D_2O}
4c[b]	(1.44 ± 0.3) × 10^{-3}	56 ± 10	6.91 ± 0.03	3.75[c]
1c	(2.37 ± 0.44) × 10^{-5}	1.08 ± 0.16	6.26 ± 0.4	1.88[d]
2c	(5.38 ± 0.79) × 10^{-5}	3.65 ± 0.38	6.75 ± 0.4	2.16[d]
3c	(6.90 ± 0.96) × 10^{-5}	1.58 ± 0.19	6.58 ± 0.4	2.32[d]

[a] T = 37 °C; k_{obsd} averages of two to three determinations for each pH. [b] Reference 18b. [c] Determined at pH 8.2. [d] Determined at pH 8.0.

data for **1c–4c** are computer-generated fits of the data to eq 7 which describes the minimum reaction scheme involving a general-base role for the imidazole (eq 8 and 9). The data obtained

$$k_{obsd} = (k_1 K_a^{Im} + k_2 K_a^{Im} K_w / [H^+]) / (K_a^{Im} + [H^+]) \quad (7)$$

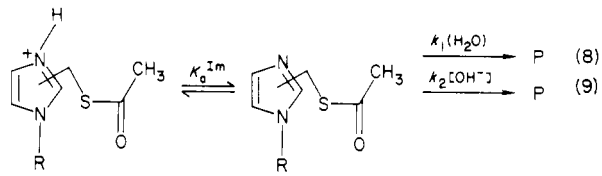

(8)

(9)

for the individual equilibrium and rate constants are given in Table VII. Each of **1c–3c** (as well as **4c**[18b]) displays a broad plateau region between pH 6.5–7 and pH 9. On the basis of the significant solvent kinetic isotope effect (k_{H_2O}/k_{D_2O} = 1.9–2.3, pH 8.0), the plateau region is most easily accounted for on the basis of a general-base delivery of H_2O by the imidazole to the thiol ester as was the case for **4c**.[18b] However, before proceeding, we must consider in more detail the nature of the species in solution in order to rule out S → *N*-acyl transfer as being an important process in hydrolysis particularly since this is the dominant process for all previously reported examples[14] which are structurally similar to those here.

Shown in Scheme III is a more detailed representation of the possible species existing in solution prior to hydrolysis. For **1c** and **2c** (R = H), all species are possible, while for **3c** (R = CH_3) species **9** and **11** cannot be formed. In order to assess the importance of S → *N*-acyl transfer, we need to estimate the value of $K_{eq} + K_{eq}'$. This can be done by a trapping experiment akin to that employed by Heller et al.[14c] whereby Ellman's reagent (5,5′-dithiobis(2-nitrobenzoic acid) (DTNB)) is used to scavenge free thiol(ate) as it is formed during the S → *N*-acyl transfer. Such an experiment can be kinetically analyzed in terms of eq

(37) (a) Fedor, L. R.; Bruice, T. C. *J. Am. Chem. Soc.* **1965**, *87*, 4138. (b) Patterson, J. F.; Huskey, W. P.; Venkatasubban, K. S.; Hogg, J. C. *J. Org. Chem.* **1978**, *43*, 4935.

(38) Bender, M. L.; Brubacher, L. J. *J. Am. Chem. Soc.* **1966**, *88*, 5880.

(39) (a) Jencks, W. P.; Carriuolo, J. *J. Biol. Chem.* **1959**, *234*, 1272. (b) Huskey, W. P.; Hogg, J. L. *J. Org. Chem.* **1981**, *46*, 53. (c) Oakenfull, D. G.; Jencks, W. P. *J. Am. Chem. Soc.* **1971**, *93*, 178–188.

Scheme III

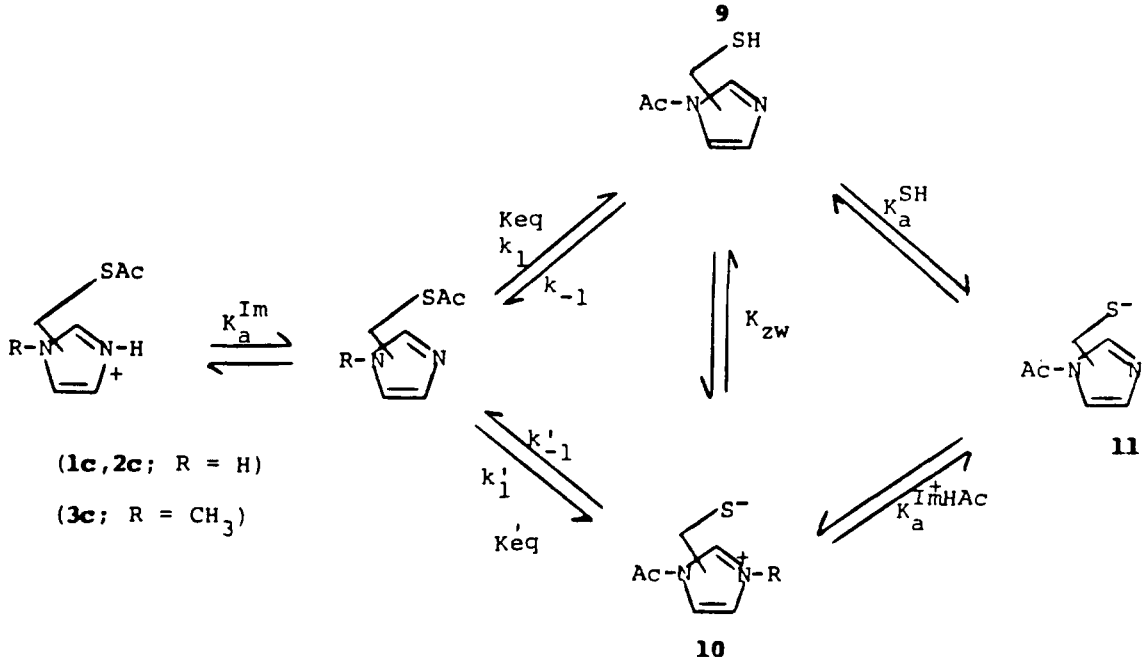

Table VIII. Observed Pseudo-First-Order Rate Constants (k_{obsd}) for Appearance of Thiolate Anion **12** Determined at pH 7.9[a]

compd	[DTNB], M	k_{obsd}, s^{-1}
2c	0[b]	4.83×10^{-5}
(9.7×10^{-4} M)	1.26×10^{-3}	7.78×10^{-4}
	4.21×10^{-3}	1.87×10^{-3}
	4.21×10^{-3}	1.79×10^{-3}
	8.42×10^{-3}	1.79×10^{-3}
	1.23×10^{-2}	1.85×10^{-3}
3c	0[b]	6.04×10^{-5}
(4.86×10^{-4} M)	4.59×10^{-3}	$(8.2 \pm 0.4) \times 10^{-5}$
	9.28×10^{-3}	$(7.6 \pm 0.4) \times 10^{-5}$

[a] T = 37 °C, aqueous solution. Errors ±5% unless otherwise stated. [b] k_{obsd} refers to the rate constant for production of RS(H) so when Ellman's reagent is not present, the value is identical with the spontaneous hydrolysis rate constant for **2c** and **3c**.

10 and 11 where k_{obsd} is the observed pseudo-first-order rate constant for the appearance of the thiolate anion **12**. Given in

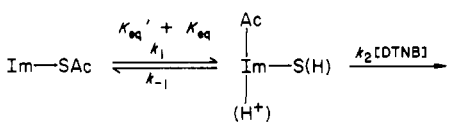

9-11

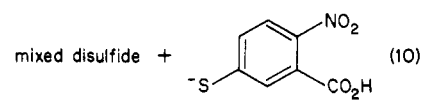

12 (10)

$$k_{obsd} = \frac{k_1 k_2 [DTNB]}{k_{-1} + k_2 [DTNB]} \quad (11)$$

Table VIII are the k_{obsd} values as a function of [DTNB] with thiol esters **2c** and **3c** determined at pH 7.9. In effect, k_{obsd} represents the sum of the rate constants for production of S(H) by normal hydrolysis and S → *N*-acyl transfer. For **2**, k_{obsd} approaches a limiting value of $\sim 1.8 \times 10^{-3}$ s^{-1} which can be taken as a reasonable measure for k_1, the rate constant for acyl transfer. Since (in eq 11) $k_{-1} = k_2$[DTNB] at one-half the limiting value for k_1 (i.e., 9×10^{-4} s^{-1}), k_{-1} can be calculated from a knowledge of k_2 ($\sim 10^5$ M^{-1} s^{-1})[40] and [DTNB] (1.5×10^{-3} M), yielding a value of 1.5×10^2 s^{-1}. Thus, $K_{eq} = k_1/k_{-1} \simeq 1.2 \times 10^{-5}$, suggesting that little *N*-acyl material is present. For the *N*-methyl derivative **3c**, there is a large uncertainty in k_{obsd} since the reactions are quite slow and the solutions have a high optical density. Nevertheless, k_1 can be at most $1.5\text{–}2 \times 10^{-5}$ s^{-1}. By the same token, k_{-1} should be, if anything, much greater than 150 s^{-1}, since the back reaction for **3c** involves neutralizing charged species.[14a] Hence, for **3c**, $K_{eq} < 2 \times 10^{-5}/1.5 \times 10^2 \simeq 1 \times 10^{-7}$. Again this points to little N-acylated material being present in solution, a result which was also obtained for **4c**.[18b]

The fact that the K_{eq} values for all **1c–4c** are small does not necessarily rule out the reaction pathway in the plateau region where most of the hydrolysis occurs by H_2O attack on **9** or **10** (Scheme III). However limits can be placed upon how rapidly those materials would have to be attacked by H_2O in order to account for the rate observed. The pseudo-first-order rate constants for H_2O attack on *N*-acetylimidazole and *N*-acetylimidazolium are reported to be[39c] 1×10^{-4} and 5×10^{-2} s^{-1}, respectively. These can be taken as base values for how rapidly **9** and **10** would hydrolyze in the absence of assistance by the adjacent S(H). S → *N*-acyl transfer from **3c** can only yield **10**, and from $K_{eq}' < 10^{-7}$, a minimum value of 1.2×10^4-fold is calculated for the required acceleration of H_2O attack on the acetylimidazolium unit by the intramolecular S^-. The fact that **2c** and **3c** follow essentially the same pH vs. log k_{obsd} profiles suggests that they hydrolyze by similar mechanisms. Hence, **10** is the only alternative acylated material that need be kinetically considered other than the *S*-acyl form. Should a general-base role for S^- actually be occurring in the zwitterionic materials one expects that increasing thiol pK_a in the series leads to a higher rate provided that the K_{eq} values are taken into account. Previous study[18b] showed that K_{eq} for **4c** $\simeq 10^{-5}\text{–}10^{-6}$ (less than for **2c** but greater than for **3c**) and that the thiol pK_a in the zwitterionic form of **4** corresponding to **10** is at least 2 units lower than for any of the similar structures for **1–3**. Nevertheless, **4c** hydrolyzes 20–

(40) (a) Semenow-Garwood, D.; Garwood, D. C. *J. Org. Chem.* **1972**, *37*, 3804. (b) Whitesides, G. M.; Lilburn, J. E.; Szajewski, R. P. *J. Org. Chem.* **1977**, *42*, 332. (c) We have determined that in 33% ethanol–H_2O, T = 36.5 °C, the second-order rate constant k_2 for attack of **4a** on Ellman's reagent is 1.70×10^4 M^{-1} s^{-1}. However, Whitesides et al.[40b] has reported that the β value for attack of thiols on DTNB is 0.36. If this value is used, the change in pK_a of the thiol (pK_1 in Table IV) from 3.9 to 6.5–8 as might be anticipated for *N*-acyl derivative **9** should increase k_2 to between 1.4×10^5 and 5.1×10^6 M^{-1} s^{-1}. Further experiments are being performed to establish these numbers more clearly.

50-fold faster than **1c–3c** which is inconsistent with a general-base role for the thiolate in **10** since the thiol having the lowest pK_a (the atomatic one) should be a weaker, not stronger, base. In fact, due to steric compression, all kinetic terms for H_2O and OH^- attack on **6** (which can be taken as a model for N-acylated **4a**) are roughly 100-fold slower than those for *N*-acetylimidazole and suggest that **10** cannot be invoked to explain the more rapid hydrolysis of **4c** than **1c–3c**. The hydrolytic data for **1c–4c** are better explained on the basis of relative leaving group abilities of the departing thiolate.

Hupe and Jencks[26] have studied the dependence of reaction rate on basicity for the reactions of thiol and oxyanions with oxygen and sulfur esters. For the reaction of alkoxide with acetylthiol esters, if attack is rate-limiting, the Brønsted β values for the nucleophile (OR^-) and leaving group (RS^-) are, respectively 0.2 and −0.4. If we consider the pathway exemplified in eq 12 for

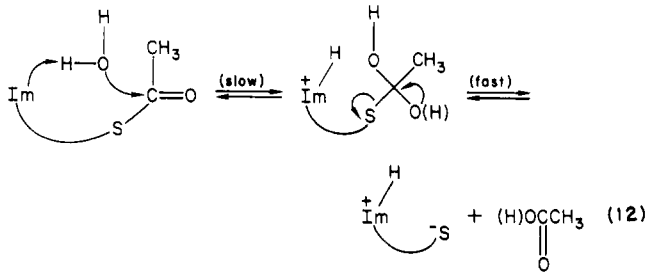

(12)

deacylation, and the general-base-delivered H_2O is the attacking nucleophile in the rate-limiting step, then the concomitant proton transfer to the imidazole has the net effect of reducing, by electrostatic means, the pK_a value of the thiol(ate) leaving group. This in turn accelerates the attack relative to a system where the cooperative ImH^+ stabilization does not occur. If we are allowed to use pK_1 in Table IV as an approximate measure of the appropriate pK_a of the thiol in this process, then a Brønsted β value of −0.48 (r = 0.992) can be calculated for the sensitivity of k_1-(H_2O) deacylation on zwitterionic thiol(ate) pK_a. Although H_2O is not fully anionic, it does possess (−) charge in the transition state. A corresponding β value of −0.48 (r = 0.962) can be calculated for OH^- attack on the thiol esters **1c–4c** by using the pK_a^{SH} values from Table IV, these being the best estimate of the state of ionization in the pH range where OH^- attack is prominent. (**Note Added in Proof**: From the above, this apparently simple intramolecular general-base catalysis has at least three benefits: (1) increasing the nucleophilicity of the attacking H_2O; (2) increasing the electrophilicity of the thiol ester C=O; (3) increasing the leaving group ability of the departing thiolate anion.)

We see no reason not to invoke a common mechanism of hydrolysis of **1c–4c**. From the above, the clearest interpretation of the rate profiles for all the cases is that given in eq 8 whereby at neutrality the deprotonated imidazole is capable of functioning as a general base in delivering H_2O to the thiol ester. This conclusion contrasts that given by Schneider[15d] who detected only a hydroxide term in the decomposition of **1c** (k_{OH} = 0.16 M^{-1} s^{-1}, T = 24 °C, pH 11.0).

IV. Conclusions and Speculations

a. Deacylation. Our original premise[18b] that the relatively slow general-base-catalyzed deacylation of **4c** stemmed from a nonideal fit of H_2O between the imidazole *N*- and *S*-acyl groups appears not to be a major factor. The overriding influence appears to be a result of the pK_a values of the RSH unit, lower values leading to faster rates. Although not as rapid as the best deacylation rate constants reported for papain (3–46 s^{-1} [1a]), hydrolysis of **4c** proceeds nearly as fast as what might be expected for the deacylation of acetylpapain, although the latter rate constant has not, to our knowledge, been reported. The estimation is based on the fact that *trans*-cinnamoylpapain deacylation occurs with a rate constant of 3.68 × 10^{-3} s^{-1},[38] while that for *trans*-cinnamoylchymotrypsin is 1.25 × 10^{-2} s^{-1}.[41] Acetylchymotrypsin is reported to deacylate about 2-fold faster, the rate constant being 2.5 × 10^{-2} s^{-1}.[42] Since neither of these acyl units can be considered ideal or even reasonable approximations to naturally occurring acyl moieties, which generally incorporate a peptide fragment, the small enhancement of the acetyl over the cinnamoyl rate of deacylation may be a result of the greater electrophilicity of the former.[43] Since the similarity of oxygen nucleophilic attack holds in general for oxygen and thiol esters,[12,26,36a] one might estimate that the deacylation rate constant for acetylpapain is on the order of 1–2 × 10^{-2} s^{-1}. If one accepts the above arguments, then in comparing the deacylation of **4c** with simple acyl-enzymes, the *N*-acyl derivative need not be invoked to explain the thiol ester hydrolysis. The faster deacylation of more ideal substrates may be attributable to other unique features such as configurational distortion provided by binding which activates the thiol ester intermediate. This interpretation contrasts but does not necessarily obviate that given by Heller et al.[14c] and Fife and DeMark[14a] who suggested a nucleophilic role for imidazole on the thiol ester rather than a general-base role in the deacylation of the cysteine proteases. However, for this to occur, some conformational change is required after acyl transfer to prevent the reacylation of cysteine.

b. Acylations. The above account shows that in systems where the relative pK_a values of a thiol and imidazole unit approach each other, a large proportion of zwitterionic material is present at physiological pH. Furthermore, this form is nucleophilically active toward *p*-NPA. Given the relatively small β value of 0.27 for rate-limiting thiol(ate) attack on *p*-NPA,[26] a considerable reduction in RS^- basicity which is obtained in passing from anionic to zwitterionic form yields only a modest reduction in nucleophilicity. Although these studies were conducted in aqueous solutions which may, by solvation, attenuate the electrostatic stabilization of the ImH^+–S^- form, the relatively hydrophobic interior of the enzyme[1] may lead to even greater amounts of the zwitterionic form over a larger pH range.

Acknowledgment. We gratefully acknowledge the financial assistance of the University of Alberta and Natural Sciences and Engineering Research Council of Canada. In addition, we acknowledge the Alberta Heritage Medical Research Foundation for a postdoctoral fellowship to J.P.S.

Supplementary Material Available: Tables of H coordinates, torsional angles, and structure factors (8 pages). Ordering information given on any current masthead page.

(41) Bender, M. L.; Schonbaum, G. R.; Zerner, B. *J. Am. Chem. Soc.* **1962**, *84*, 2540.
(42) Gutfreund, H.; Sturtevant, J. M. *Biochem. J.* **1956**, *63*, 656.
(43) For example k_{OH}[*p*-NPA]/k_{OH} [*p*-nitrophenylcinnamate] = 15 M^{-1} s^{-1}/2.85 M^{-1} s^{-1} = 5.26 (from data in: Edwards, J. O.; Pearson, R. G. *J. Am. Chem. Soc.* **1962**, *84*, 16. Bender, M. L.; Zerner, B. *Ibid.* **1962**, *84*, 2550).